Journal of Peptide Science
J. Peptide Sci. **8**: 211–226 (2002)
Published online in Wiley InterScience (www.interscience.wiley.com). DOI: 10.1002/psc.384

Conformational Solution Studies of Neuropeptide γ Using CD and NMR Spectroscopy

SYLWIA RODZIEWICZ-MOTOWIDŁO,[a]* KRZYSZTOF BRZOZOWSKI,[a] ANNA ŁĘGOWSKA,[a] ADAM LIWO,[a] JERZY SILBERING,[b] MAREK SMOLUCH[b] and KRZYSZTOF ROLKA[a]

[a] Faculty of Chemistry, University of Gdańsk, Sobieskiego 18, PL-80-952 Gdańsk, Poland
[b] Faculty of Chemistry and Regional Laboratory, Jagiellonian University, Ingardena 3, PL-30-060 Kraków, Poland

Received 7 December 2001
Revised 11 February 2002

Abstract: Neuropeptide γ is one of the largest members of the tachykinin family of peptides, exhibiting strong agonistic activity towards the NK-2 tachykinin receptor. This peptide was synthesized by the solid-phase method using the Fmoc chemistry. Circular-dichroism spectroscopy (CD) investigations of this peptide were performed in phosphate buffer, in the presence of sodium dodecylsulphate (SDS) micelles and trifluoroethanol (TFE) solutions and in DMSO-d_6 using the 2D NMR technique in conjunction with two different theoretical approaches. The first assumes multiconformational equilibrium of the peptide studied characterized by the values of statistical weights of low-energy conformations. These calculations were performed using three different force fields ECEPP/3, AMBER4.1 and CHARMM (implemented in the X-PLOR program). The second method incorporates interproton distance and dihedral angle constraints into the starting conformation using the *Simulated Annealing* algorithm (X-PLOR program). The CD experiments revealed that although the peptide studied is flexible in polar solvents, a tendency to adopt a helical structure was observed in the hydrophobic environment. The NMR data (NOE effects) indicate a helical or reverse structure in the Ile7–His12 fragment of the peptide studied in DMSO-d_6 solution. The results obtained cannot be interpreted in terms of a single conformation. Most of the conformations obtained with the ECEPP/3 force field possess a high content of a helical structure. None of the conformers, obtained with the AMBER4.1 and CHARMM force fields, can be considered as the dominant one. In all conformations several β-turns were detected and in some cases γ-turns were also found. But in fact, it is rather difficult to select the position of the secondary element(s) present in the structure of NPγ in solution. All conformers calculated with the X-PLOR program (with using NMR derived distance and torsion angle constraints) are stabilized by several β-turns. Common structural motives are a type IV β-turn in the Gln6–His12 fragment. All conformations obtained using two approaches adopt very similar turn shapes in the middle region of molecule and a random structure on the *N*- and *C*-terminal fragments.

Keywords: conformational studies; tachykinins; neuropeptide γ; NMR spectroscopy; CD spectroscopy; conformational analysis conformational equilibrium Monte Carlo methods; molecular dynamic

INTRODUCTION

Neuropeptide γ (NPγ) was isolated for the first time in 1988 from rabbit intestine by Kage *et al.* [1]. It appeared to be a naturally occurring tachykinin family peptide displaying preferable agonistic activity towards the NK-2 tachykinin receptor. NPγ contains neurokinin A(NKA) as its *C*-terminal decapeptide and forms the 16–34 fragment of NPK. As demonstrated by several groups [2–4], NPγ possesses a higher affinity towards NK-2 tachykinin than neurokinin A — a 'classical' mammalian agonist of this receptor.

* Correspondence to: Dr S. Rodziewicz-Motowidło, Faculty of Chemistry, University of Gdańsk, Sobieskiego 18, PL-80-952 Gdańsk, Poland; e-mail: sylwia@chemik.chem.univ.gda.pl
Contract/grant sponsor: Polish State Committee for Scientific Research; Contract/grant number: PB463/709/97/13.

The amino acid sequence of this peptide is as follows: Asp^{1}-Ala-Gly-His-Gly-Gln-Ile-Ser-His-Lys-Arg-His-Lys-Thr-Asp-Ser-Phe-Val-Gly-Leu-Met^{21}-NH_2. Extensive studies provided the evidence that NPγ is involved in many biological activities, e.g. it was found to be the most potent contractile tachykinin in human isolated bronchus (10-fold more potent than NKA) [5]. Therefore research connected with this peptide may determine the molecular mechanism responsible for respiratory-system diseases, e.g. asthma and it may also help in obtaining analogues with potential therapeutic significance.

NMR conformational studies of NK-2 agonists led to several solution conformations. Early works of Chassaing *et al.*, [6] indicated that the structure of NKA in water is flexible, with a salt bridge at the *N*-terminal fragment formed between the Lys2 and Asp4 side chains. Moreover, the authors did not find any NKA conformation containing any secondary structure elements in organic solvents [6]. However, another group [7] based on the NOEs effects suggested that a series of dynamic turns in equilibrium are present in the 3–10 fragment in TFE solutions. The structure becomes more ordered when TFE is titrated into water solution. The conformational NMR study of a more selective NK-2 agonist NKA(4–10) revealed that this peptide is characterized by a structure containing a type I β-turn in the 5–8 fragment, followed by a γ-turn centred on Gly8 in DMSO-d_6 solutions [8]. In the case of an even more active and more selective analogue [β-Ala^{8}]NKA(4–10), the first β-turn is followed by a C_8 turn comprising β-Ala8 and Leu9 and by another β-turn extending from β-Ala8 to the *C*-terminal NH_2 group [8]. A recent study [9] of NKA in the presence SDS-d_{25} micelles indicated that under these conditions the peptide adopts an α-helical structure in the 6–9 fragment, and the length of this secondary structure element is responsible for the binding potencies towards tachykinin receptors.

Taking into consideration the findings discussed above, we decided to investigate the structure of NPγ in solution. First, it is a more selective NK-2 agonist than the peptides already studied. In addition, NPγ has a much longer chain. The common problem with conformational studies of short, linear peptides is that their conformational flexibility does not allow results to be interpreted in terms of a single conformation. In fact, the calculated solution conformations of such peptides might represent the 'average' conformation of those existing under the conditions applied for the experiment. One can assume that investigations of longer peptides (such as this 21-residue peptide), although more complicated, might (for the reason discussed above) yield a more definite resolution of the structure, which is more likely to be similar to the bioactive one.

In this paper we describe a conformational study of NPγ using the CD method and 2D NMR spectroscopy combined with theoretical conformational analysis. The first method gives information on the average conformation of the peptide in different solvents in a short time, whereas the second approach, NMR spectroscopy in conjunction with the theoretical calculations, allows the determination of probable conformations of the peptide in solution.

MATERIALS AND METHODS

Peptide Synthesis

NPγ was synthesized by the solid-phase method using Fmoc chemistry. The TentaGel S RAM (substitution of Fmoc groups 0.22 meq/g) (RAPP Polymere, Germany) was used as a support. The synthesis of the *C*-terminal nonapeptide was carried out on an automatic synthesizer (Applied Biosystems, model 430A). In order to control the coupling efficiency, starting from His13 the synthesis was completed manually. During the synthesis the following amino acid derivatives were used: Fmoc-Gly, Fmoc-Ala, Fmoc-Leu, Fmoc-Ile, Fmoc-Val, Fmoc-Phe, Fmoc-Met, Fmoc-Ser(tBu), Fmoc-Thr(tBu), Fmoc-Asp(OtBu), Fmoc-Gln(Trt), Fmoc-His(Trt), Fmoc-Arg(Pbf), Fmoc-Lys(Boc). Deblockings were performed with 20% piperidine in DMF–NMP (1 : 1, v/v) with the addition of 1% Triton X-100. Couplings were achieved using 1 M solutions of HOBt — DIC (1 : 1, v/v) in a mixture of DMF–NMP (1 : 1, v/v) with the addition 1% Triton X-100 for 60 min or HOBt/TBTU/DIPEA (molar ratio 1 : 1 : 2) in the mixture DMF–DCM (1 : 1,v/v). After synthesis had been completed, the peptide was removed from the resin together with the side chain protections in a one-step procedure using TFA — phenol — triethylsilane — H_2O (88 : 5 : 2 : 5), v/v) [10]. The crude peptide was purified by gel filtration on a Sephadex G-15 column using 50% acetic acid as an eluent. Further purification was carried out on a semipreparative C18 HPLC column (Vydac, ODS 10 × 250 mm, 10 μm) in a linear gradient 10%–60% B for 40 min (A: 1% TFA in water;

B: 80% acetonitrile in A). The purity of the peptide was higher than 98% as judged by HPLC analysis (R_t = 11.5 min; analytical column Vydac, ODS 4.6 × 200 mm, 5 μm; in a linear gradient 10%–60% B for 40 min). The peptide showed the correct molecular mass as measured by mass spectroscopy using the ESI-MS technique.

CD Experiment

For CD measurements, NPγ solutions were prepared by weight from lyophilized material. The peptide concentration was 0.23 mM. CD spectra were obtained at room temperature on a Jasco J-20 spectropolarimeter automated and equipped with a program prepared by Medson (Poland). Quartz cells of 1–5 mm were used. The results were plotted as the mean residue ellipticity $[\Theta]_r$ [degree × cm^2 × dmol^{-1}]. Trifluoroethanol (TFE) was of spectroscopic quality, 0.1 M phosphate buffer was prepared from the purest reagents. 1-Dodecylsulphate sodium salt (SDS) was of analytical grade.

NMR Experiment

For NMR measurements the peptide was dissolved in a 0.5 ml DMSO-d_6. The peptide concentration was 25 mM. All experiments were performed on a Varian Unity 500 Plus spectrometer (Varian Instruments, USA), operating at a 500 MHz resonance frequency. All spectra were recorded at 303 K. For the two-dimensional experiments, the time-domain matrices consisted of 4096 × 128 complex data points for the ACT-ct-COSY [11], 2048 × 310 for the TOCSY [12], ROESY [13], NOESY [14], and were zero filled to obtain a frequency domain matrix of 4096 × 2048 complex data points with a spectral width of 4785.8 Hz for the ACT-ct-COSY, 2048 × 2048 with a spectral width of 4878.6 Hz for the TOCSY, ROESY and NOESY. For the heteronuclear experiments, HMQC [15] and HMBC [16], 2432 × 230 time data matrices were zero filled to 2048 × 1024 with a spectral width of 4822.7 Hz in F1 (^{13}C) and 21998.2 Hz in F2 (^{1}H). A mixing time of 400 ms was used for the NOESY, 200 ms for the ROESY and 90 ms for the TOSCY spectra. The TOCSY and ROESY spectra were recorded in the phase-sensitive mode. All data were processed and cross-peak volume calculations were performed with the XEASY program [17] on the SUN Ultrasparc workstation.

The assignment of the proton resonances was accomplished based on the TOCSY, NOESY, HMBC and HMQC spectra. The spin systems of Leu20 and Val18 were identified based on the position and shape of the signals of methyl protons H$^\delta$ and H$^\gamma$, respectively. The spin systems of Lys10, Arg11 and Lys13 were unambiguously identified by their characteristic spin coupling patterns of methylene protons of H$^{\beta,\gamma,\delta}$ with H$^{\varepsilon,\eta,\xi}$ protons. Met21 was identified by its characteristic proton spin system of H$^\beta$ and H$^\gamma$. Phe17 proton signal assignment was possible with the use of NOE cross-peaks of the H$^\beta$ and aromatic protons. Similarly NOE cross-peaks between H$^\delta$ protons of His4, His9 and His12 and their own H$^\beta$ protons were useful for confirming resonance assignments. Thr14 was recognized by its characteristic correlation between H$^\alpha$ and H$^\beta$ protons in the α-α region. Asp1, Ala2 and Asp15 were identified based on the fact that their α protons were connected to the protons of ethylene (Asp) and methyl (Ala) groups only, respectively. The proton chemical shifts of the peptide studied are shown in Table 1.

The $^3J_{NHH\alpha}$ vicinal couplings constants were determined using a constant-time ACT-ct-COSY experiment described by Koźmiński [11]. Because of the overlapping of the signals in the amide region, only seven vicinal coupling constants were measured (Table 1). The estimated experimental error was 0.1 Hz. Torsion angles were generated using the HABAS program [18] of the DYANA package [19], on the basis of the Bystrov-Karplus equation [20].

All NOE cross-peaks, for the peptide studied, were picked up on the NOESY spectrum. The NOE volumes were integrated and calibrated with the XEASY [17] software. 281 NOE-derived restraints were manually collected. The cross-peaks obtained from the NOESY experiment were converted, after internal calibration, into upper distance limits by the CALIBA program [21]. Finally, after DYANA filtering, 196 upper limit distance constraints were conserved (95 intra-residual, 65 sequential and medium-range and 36 long range). Interproton distances were calibrated against geminal protons.

Conformational Calculations

The three-dimensional solution structure of NPγ peptide was determined by two approaches:

1. Using restrained molecular dynamics SA to obtain conformations that satisfied the experimental data, the SA protocol of the X-PLOR program was used.

Table 1 The Chemical Shifts (ppm) and Vicinal Coupling Constants ($^3J_{NHH}\alpha$) of NPγ in DMSO-d_6 at 303 K

Residue	Chemical shifts (ppm)								$^3J_{NHH}\alpha$ (Hz)
	NH	H^α	H^β	H^γ	H^δ	H^ε	others	C^α	
Asp1	n	4.09	2.85; 2.66				COOH n	49.06	—
Ala2	8.64	4.32	1.23					48.80	—
Gly3	8.17	3.73; 3.69						42	—
His4	8.13	4.58	3.11; 2.95		7.36	n	H^δn	51.47	—
Gly5	8.34	3.81; 3.71						42.12	—
Gln6	8.21	4.21	1.64; 1.48	3.07			H^ε7.72	d	8.1
Ile7	7.88	4.17	1.68	1.36; 1.01	0.76			56.96	8.0
Ser8	8.01	4.28	3.58; 3.52				H^γ n	d	8.3
His9	8.15	4.61	3.07; 2.98		7.33	8.92	H^δn	51.47	8.1
Lys10	8.23	4.29	1.52	1.33	1.67	2.75	H^ξ7.75	52.90	6.6
Arg11	8.10	4.33	1.81	1.70	2.10		H^η 6.80	52.35	—
							H^ε 7.28		—
His12	8.27	4.61	3.14; 2.94		7.30	8.29	H^δn	51.47	—
Lys13	8.02	4.21	1.62	1.30	1.49	2.74	H^ξ 7.79	d	8.4
Thr14	8.01	4.26	3.99	1.01				52.28	8.0
Asp15	8.167	4.60	2.68; 2.52				COOH 8.90	49.49	9.0
Ser16	7.78	4.26	3.48				H^γ 4.96	51.40	—
Phe17	8.06	4.54	3.05; 2.81			7.21	H^δ 7.15	54.22	9.2
Val18	7.86	4.11	1.94	0.83; 0.88				58.35	—
Gly19	8.13	3.68; 3.75						42	—
Leu20	7.91	4.27	1.59	1.45	0.82; 0.86			58.10	7.3
Met21	7.92	4.22	1.91; 1.79	2.44; 2.37				d	7.2
C-NH2	(E)n								—
	(Z)n								—

n, not observed; d, difficult to measure.

2. A global conformational search of the peptide studied using the EDMC method with the ECEPP/3 force field, the Simulated Annealing (SA) protocol with AMBER4.1 and CHARMM (as implemented in the X-PLOR program) force fields and subsequent calculation of statistical weights of the obtained conformations by fitting the theoretical NOESY spectra and vicinal coupling constants $^3J_{NHH}\alpha$ to the experimental ones.

In the first method, a classical approach using restrained molecular dynamics (with interproton distances calculated from NOE intensities and torsion angles calculated from vicinal coupling constants) to obtain conformations that satisfy experimental data was applied. The SA protocol implemented in the X-PLOR program was used. In the second method, a recently developed algorithm [22] (included in ANALYZE program) was applied allowing the interpretation of the results obtained in terms of multi-conformational equilibrium of the peptide studied. In the first stage, all low-energy conformations were found by extensive global conformational analysis using the EDMC [23] method with the ECEPP/3 [24] force field and the Simulated Annealing (SA) protocol in AMBER4.1 [25] and CHARMM force fields. Then NOE effects and vicinal coupling constants $^3J_{NHH}\alpha$ for each conformation were calculated. Finally, the statistical weights of these conformations by means of a nonlinear least-squares procedure were determined, in order to obtain the best fit of the calculated NOE effects and vicinal coupling constants $^3J_{NHH}\alpha$ to the experimental NMR data.

X-PLOR3.1 Simulated Annealing Simulations

The standard modules of Simulated Annealing algorithm of the X-PLOR program [26] were used. The calculations were carried out using the CHARMM force field [27] *in vacuo* starting from a random structure. Additionally, NMR-derived constraints on

Table 2 Positions of α-Helical Fragments, β-turns and γ-turns in NPγ Conformations Computed in EDMC, Simulated Annealing in AMBER4.1 and CHARMM force fields and Simulated Annealing in X-PLOR program. In the case of approach 1 statistical weights of conformations are also given

NPγ							
EDMC ensemble		SA (AMBER4.1) ensemble		SA (X-PLOR)ensemble		SA (X-PLOR)structures	
α-helix His12-Met21	62.0%	Ala2-Gly3 type I Gly5 inversed γ-turn	9.3%	Ala2-Gly3 type IV His4-Gly5 type II Ile7-Ser8 type I Ser8-His9 type I	9.6%	Ile7-Ser8 type IV Ser8-His9 type IV His9-Lys10 type IV Lys10-Arg11 type VII Ser16 Phe17 type IV	Family 1
α-helix Gln6-Met21	38.0%	Lys13-Thr14 type III Thr14-Asp15 type III Asp15-Ser16 type III Gly 3 inversed γ-turn	7.2%	Gly3-His4 type I' His4-Gly5 type I' Ser8-His9 type I' Lys10-Arg11 type IV Phe17-Val18 type III Gly19-Leu20 type II' Gly 5 γ-turn	6.5%	His4-Gly5 type IV Gly-Gln6 type VII Ile7-Ser8 type IV Ser8-His9 type VII His9-Lys10 type IV Lys10-Arg11 type IV Lys13-Thr14 type II Ser16-Phe17 type VII	Family 2
		Ser8 γ-turn	6.5%	Gln6-Ile7 type II' Ser16-Phe17 type III	6%	Gly3-His4 type IV His4-Gly5 type IV Gln6-Ile7 type IV Ile7-Ser8 type IV Ser8-His9 type IV His9-Lys10 type IV Lys10-Arg11 type VII Lys13-Thr14 type VII Ser16-Phe17 type VII Val18-Gly19 type VII	Family 3
		His4 γ-turn	6.1%	Ala2-Gly3 type IV Gln6-Ile7 type II' His12-Lyl13 type II' Lys13-Thr14 type IV	5%	Gln6-Ile7 type IV Ile7-Ser8 type IV Ser8-His9 type IV His9-Lys10 type IV Lys10-Arg11 type IV Val18-Gly19 type VII	Family 4
		Gln6-Ile7 type III Ser8-His9 type III	5.9%		4.6%	His4-Gly5 type IV Gly5-Gln6 type IV Ile7-Ser8 type III Ser8-His9 type I His9-Lys10 type I Lys10-Arg11 type VII Asp15-Ser16 type VII	Family 5
		Gly5-Gln6 type III	5.8%	Ser8-His9 type IV Asp15-Ser16 type IV	4.5%	Ile7-Ser8 type IV His9-Lys10 type I Lys10-Arg11 type IV Arg11-His12 type I Ser16-Phe17 type IV Gly19-Leu20 type VII	Family 6
			5.5%	His4-Gly5 type I' His12-Lys13 type IV	4.1%	His4-Gly5 type IV Ile7-Ser8 type VII Ser8-His9 type VII	Family 7

(*continued overleaf*)

Table 2 (*Continued*)

			NPγ			
EDMC ensemble	SA (AMBER4.1) ensemble		SA (X-PLOR)ensemble		SA (X-PLOR)structures	
					His9-Lys10 type IV Asp15-Ser16 type IV Ser16-Phe17 type VII Gly19-Leu20 type IV	
	11Arg γ-turn	5.3%	Gln6-Ile7 type IV Lys13-Thr14 type IV Val18-Gly19 type IV Gly19-Leu20 type IV	4%	Ala2-Gly3 type IV Gly3-His4 type VII Ile7-Ser8 type IV Ser8-His9 type IV His9-Lys10 type III His12-Lys13 type VII Ser16-Phe17 type IV	Family 8
	His9-Lys10 type III Val18-Gly19 type II	4.8%	Ala2-Gly3 type I His4-Gly5 type II Gln6-Ile7 type IV Lys10-Arg11 type IV Ser16-Phe17 type II' Phe17-Val18 type IV Gly19-Leu20 type IV	3.7%	Gly5-Gln6 type IV Ile7-Ser8 type IV Ser8-His9 type IV His9-Lys10 type IV Asp15-Ser16 type IV Gly19-Leu20 type IV	Family 9
	Val18-Gly19 type II	4.6%	Ala2-Gly3 type IV Gly3-His4 type I His4-Gly5 type IV His9-Lys10 type I His12-Lys13 type III Ser16-Phe17 type IV Gly19-Leu20 type V	3.6%		
		4.3%	His9-Lys10 type IV Gly19-Leu20 type IV	3.5%		
	Ala2-Gly3 type II'	4.1%	His4-Gly5 type IV Gln6-Ile7 type II' His12-Lys13 type IV Asp15-Ser16 type I Val18-Gly19 type V	3.4%		
	Ile7-Ser8 type II	4.0%	Lys13-Thr14 type IV Gly 5 inversed γ-turn	3.3%		
	His4-Gly5 type II Lys13-Thr14 type III Thr14-Asp15 type I Gly19-Leu20 type II'	3.3%	Ala2-Gly3 type I Gly3-His4 type IV Gln6-Ile7 type I His9-Lys10 type IV Gly19-Leu20 type II'	3.2%		

interproton distances and dihedral angles, with force constants ($f = 50$ kcal/(mol $\times$ Å^2) and ($f =$ 50 kcal/mol$\times$rad^2), as well as constraints on the ω angles of the peptide group to keep them in a *trans* configuration (with the force constant 500 kcal/mol $\times$ rad^2) were added to the target function. Electrostatic interactions and energy of hydrogen bonds were not directly included and van der Waals interactions were described with the simplified potential function. The chirality of all C^{α} atoms (except for the Gly residues) was also fixed to L by imposing a three-fold potential on the N-CO-C^{α}-C^{β} improper torsion angles ($f = 500$ kcal/mol $\times$ rad^2). The search was started

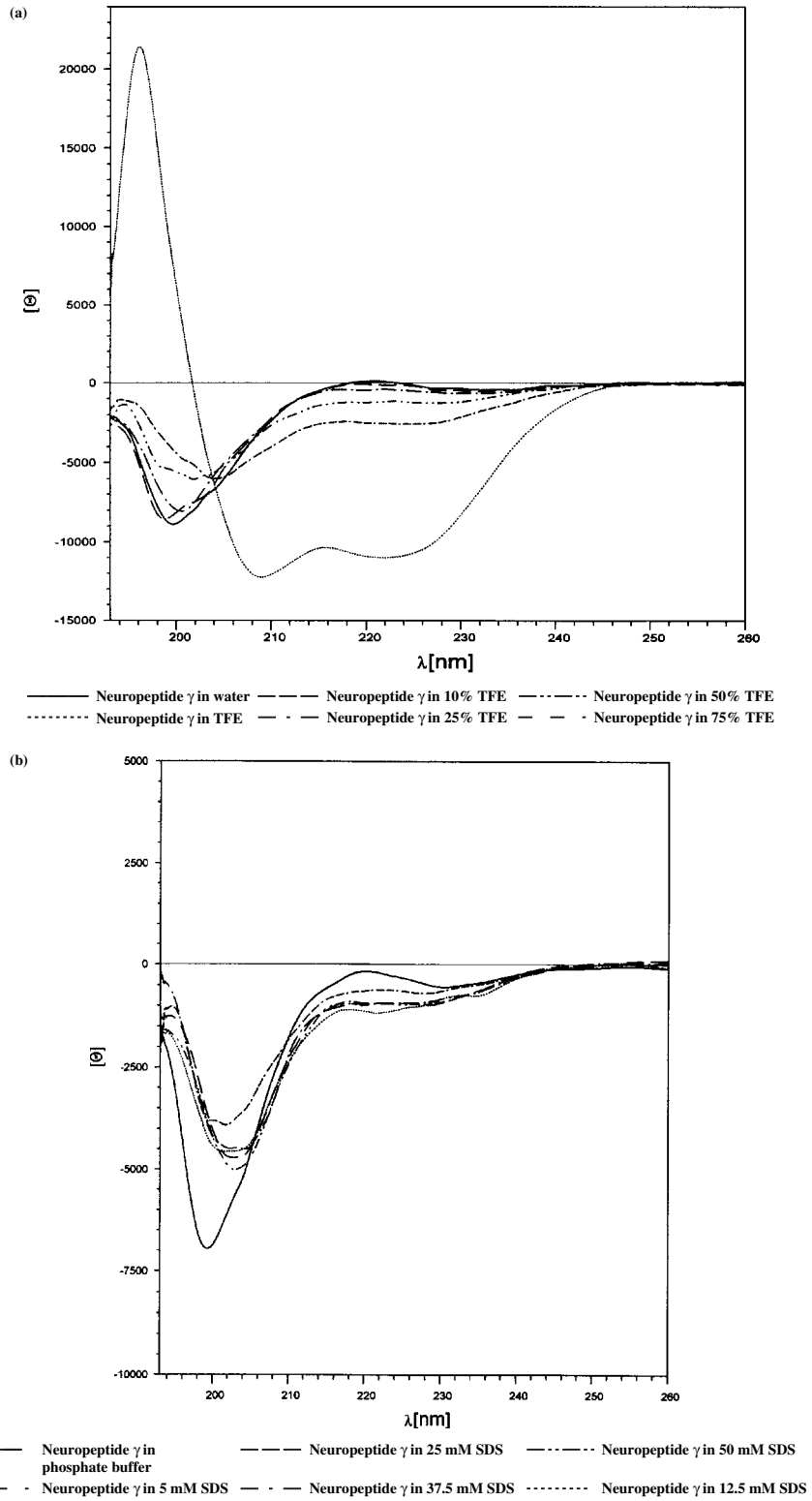

Figure 1 The CD spectra of NPγ peptide were obtained at room temperature in: (a) water; TFE; TFE in water 10%, 25%, 50%, 75%; (b) phosphate buffer pH =7; SDS (23 mM); SDS in water (0.144 mg SDS in 10 ml of water); SDS in phosphate buffer 5 mM, 12.5 mM, 25 mM, 37.5 mM, 50 mM.

from a random-generated conformation. 300 cycles of SA were carried out for the peptide studied. Each cycle included 27 000 iterations of 80 ps with the 3 fs steps. The molecule was heated at 1000 K for 50 ps and annealed at 100 K for 29 ps. In the last 200 iterations (1 ps) energy minimization with the use of the Powell algorithm [28] was performed. During SA refinement of the structure, the molecule was cooled slowly from 1000 K to 100 K for 30 ps. Finally, 300 energy-minimized conformations were obtained. The set of the final conformations was clustered (using the minimal-tree algorithm). The RMSD between heavy atoms at the optimum superposition was taken as a measure of the distance between conformations, also a cut-off value of 4.0 Å was used to separate the families. Nine families of conformations were considered in further analysis.

EDMC Calculations

The search of the conformational space of the peptide studied was first performed by the electrostatically driven Monte Carlo method (EDMC) [23]. Conformational energy was evaluated using the ECEPP/3 (Empirical Conformational Energy Program for Peptides) force field [24], which assumes rigid valence geometry. The chirality of all C^{α} atoms (except for Gly residues) was fixed to L and the geometry of the peptide bonds was fixed to *trans* according to the NMR data. The force field included a hydration contribution (E_{hydr}), which was calculated using the SRFOPT surface-solvation model of Vila *et al.* [29] with original parameters. A dielectric constant $\varepsilon = 2$ was used in the calculations, according to the recommendation of the authors of the ECEPP/3 force field [24]. The temperature parameter in EDMC simulations was 1000 K, which corresponded to a reasonable acceptance rate of 20%–30%. The software used was the ECEPPAK global conformational analysis package [30]. Finally, 3000 energy-minimized starting conformations were obtained. The set of the final conformations was clustered (using the

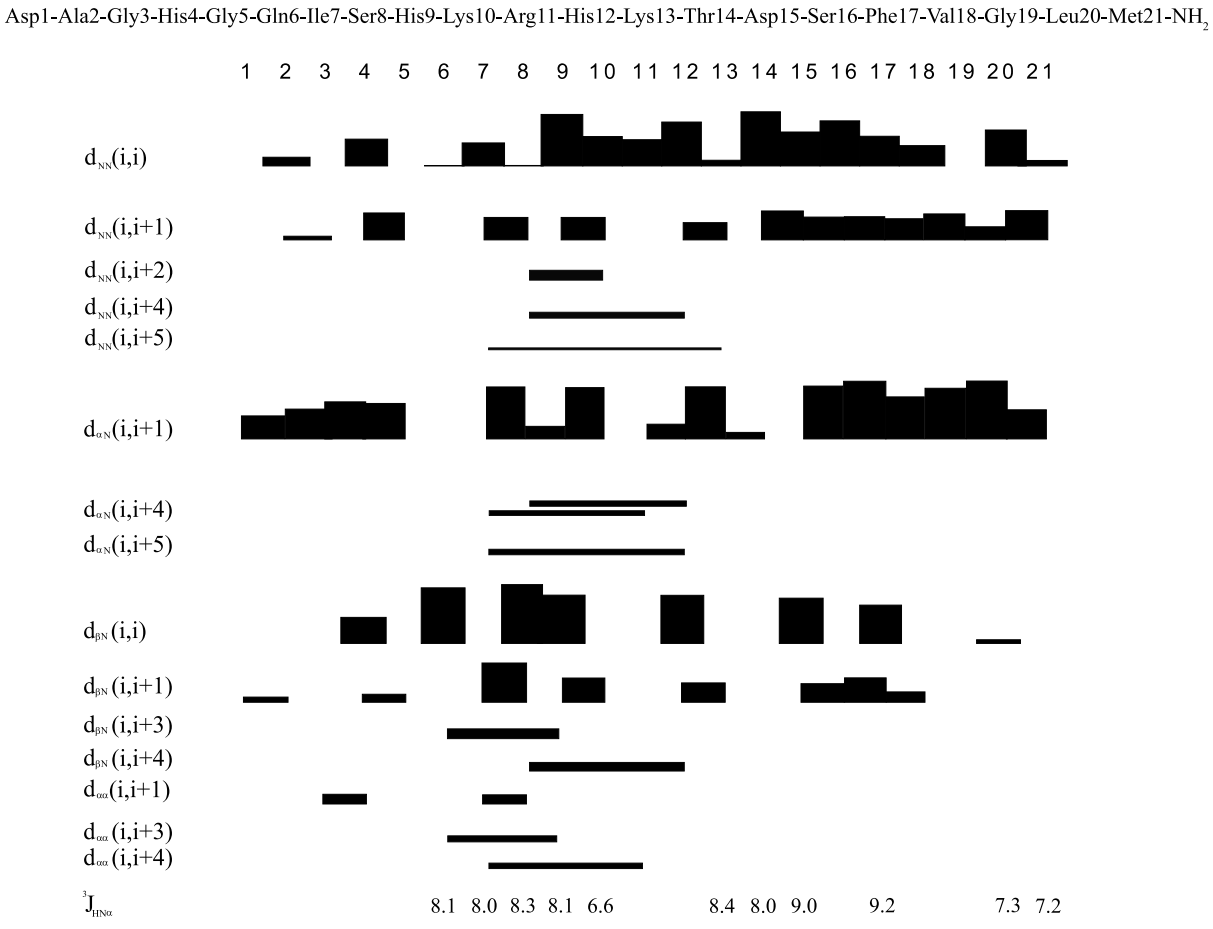

Figure 2 The integral intensities of off-diagonal signals in NOESY spectrum of NPγ in DMSO-d_6 solution.

minimum-variance algorithm [31]). The root mean square deviation (RMSD) between heavy atoms at optimal superposition was taken as a measure of the distance between conformations, and a cut-off value of 0.3 Å was used to separate the families to afford 809 families of conformations.

AMBER4.1 Simulated Annealing Simulations

The calculations were carried out using the AMBER4.1 force field [25] *in vacuo*. According to the NMR data (NOE effects), the geometry of the peptide group was fixed to *trans* by imposing

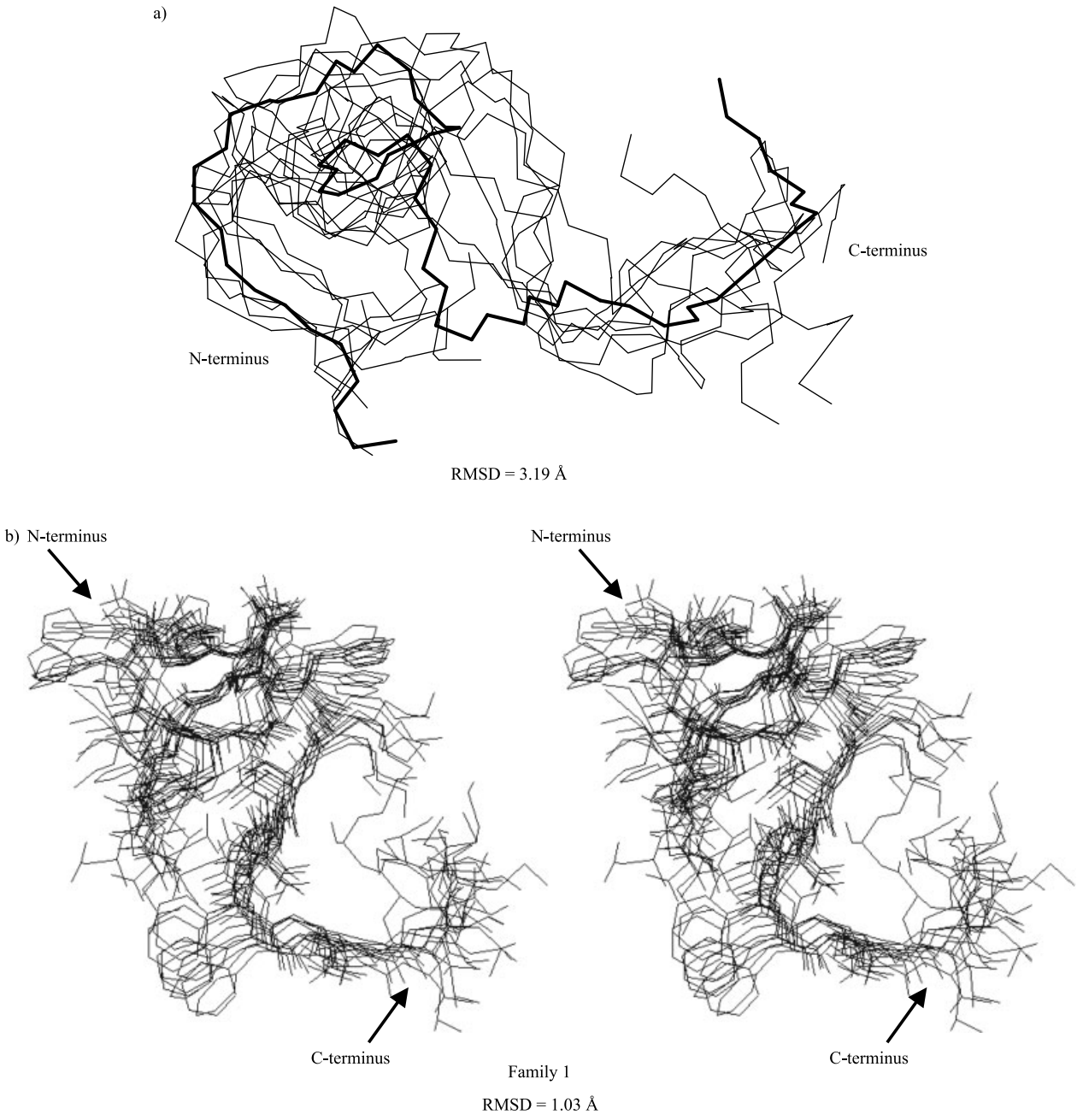

Figure 3 (a) Superposition of the lowest energy conformations from each family of NPγ molecule obtained in the X-PLOR program for all α-carbon atoms (RMSD = 3.19 Å). Backbone of the lowest energy conformation is represented by the bold line. (b) Stereoview of superposition of 10 of the lowest energy (Family 1) conformations of NPγ molecule obtained in the X-PLOR program in whole α-carbon atoms (RMSD = 1.03 Å).

harmonic constraints with force constants of f = 100 kcal/mol × rad^2 on the corresponding ω angles. Also the chirality of all C$^\alpha$ atoms (except for the Gly residues) was fixed to L (f = 30 kcal/mol × rad^2). The starting conformation was set to an α-helix. In the Simulated Annealing algorithm the molecule was heated to 1200 K for 3000 fs and annealed at 273 K for 12 000 fs with 10 cycle runs. The ramping method (linear ramping) was applied for the annealing. For further calculations the lowest energy structures were selected, and the energy minimization step (10 000 cycles) was again performed using the AMBER4.1 force field. Finally, 1000 energy-minimized conformations were obtained. The set of the final conformations was not clustered into families.

CHARMM Simulated Annealing Simulations

The same method as described above was used in the case of generating conformational ensemble using the X-PLOR program, but without constraints put on distances and angles. All other aspects of the simulation are described in the X-PLOR3.1 program (Simulated Annealing simulations algorithm) [26]. The aim of this calculation was the comparison of the results obtained with those from the AMBER4.1 force field.

Calculation of the Statistical Weight of the Conformations by Fitting the Theoretical to the Experimental NMR Data

In the next step of the analysis, the intensities of NOE effects and the $^3J_{\mathrm{NHH}}\alpha$ vicinal coupling constants for all conformations (obtained in the AMBER4.1 and CHARMM force fields) and for the lowest energy conformations (from each family obtained in ECEPP/3 force field) were calculated. The intensities of NOE effects were computed by solving the system of the Solomon differential equations [32] applying the MORASS2.1 program [33,34]. The vicinal $^3J_{\mathrm{NHH}}\alpha$ coupling constants of low-energy conformations were calculated from the empirical Bystrov-Karplus relationship [20]. Based on the sets of measured and theoretically calculated observables, the statistical weights of the conformations were fitted to obtain the best agreement between the theoretical and experimental values of the NMR observables, using the algorithm developed in our earlier work [22]. The theoretical values are defined as averages over conformations [Eqn. (1)–(3)]

$$\overline{V}_i = V_0 \sum_{j=1}^{NC} x_j v_{ji} \quad i = 1, 2, \ldots, NP \tag{1}$$

$$\overline{J}_i = \sum_{j=1}^{NC} x_j J_{ji} \quad i = 1, 2, \ldots, N\Theta \tag{2}$$

$$\text{with} \sum_{i=1}^{NC} x_i = 1 \tag{3}$$

where V_i is the calculated average intensity of ith NOE signal, v_{ji} is the intensity of ith signal calculated for jth conformation, V_0 is a scaling factor, J_i is the ith calculated average coupling constant, J_{ji} is the ith coupling constant calculated for jth conformation, NP is the number of NOE signals, $N\Theta$ is the number of the coupling constants, NC is the number of conformations and x_i, $i = 1, 2, \ldots, NC$ are the statistical weights of the respective conformations. Poor-quality NOEs and the NOEs of uncertain assignment were not considered in fitting the statistical weights. The target function is by Eqn. (4) [22].

$$\begin{aligned} \min \Phi = & \sum_{k=1}^{NV} w_k (\overline{V_k^{calc}} - \overline{V_k^{\exp}})^2 \\ & + w_J \sum_{k=1}^{N\theta} (\overline{J_k^{calc}} - \overline{J_k^{\exp}})^2 \\ & + \sum_{k=1}^{NJ} \left(\frac{A_k - A_k^0}{\sigma_{A_k}} \right)^2 + \left(\frac{B_k - B_k^0}{\sigma_{B_k}} \right)^2 \\ & + \left(\frac{C_k - C_k^0}{\sigma_{C_k}} \right)^2 \end{aligned} \tag{4}$$

where the superscript *exp* marks the measurement quantity, w_i is the weight of the ith NOE, w_J is the weight of the coupling-constant term, A_k, B_k and C_k are the constants in the Karplus equation [20], the superscript 0 denoting the standard values, and σ_A, σ_B and σ_C are the estimated standard deviations of constants. Including the deviations of the constants in the Karplus equation from the average values enables us to take into account the fact that this relationship is empirical and the coefficients are subject to error. We used $w_J = 0.1$ Hz^{-2} and $\sigma_A = \sigma_B = \sigma_C = 2$ Hz. The weights of the NOE intensities were calculated from Eqn. (9) of [22]. Although the weights of the respective least-square terms cannot be established unequivocally, we have shown previously that the calculated populations of conformations ($x_1, x_2, \cdot, x_{NC}$) are not very sensitive on these

parameters. However, the populations are sensitive on the basis set and it is therefore critical that the search procedure be able to find all 'reasonable' conformations. Previous work has shown that the EDMC conformational search engine [23] implemented in this study has this property. For details of the population-fitting algorithm and for detailed discussion of its properties the reader is referred to the original study [22].

Conformations with statistical weights (populations) exceeding 3% were taken to further comparative analysis. This cut-off was chosen because beyond it there were many diverse conformations with very low weights and any comprehensible analysis would be impossible. Refitting using only the conformations fulfilling this criterion did not change significantly the agreement between theoretical and calculated NOEs and $^3J_{NHH}\alpha$ values

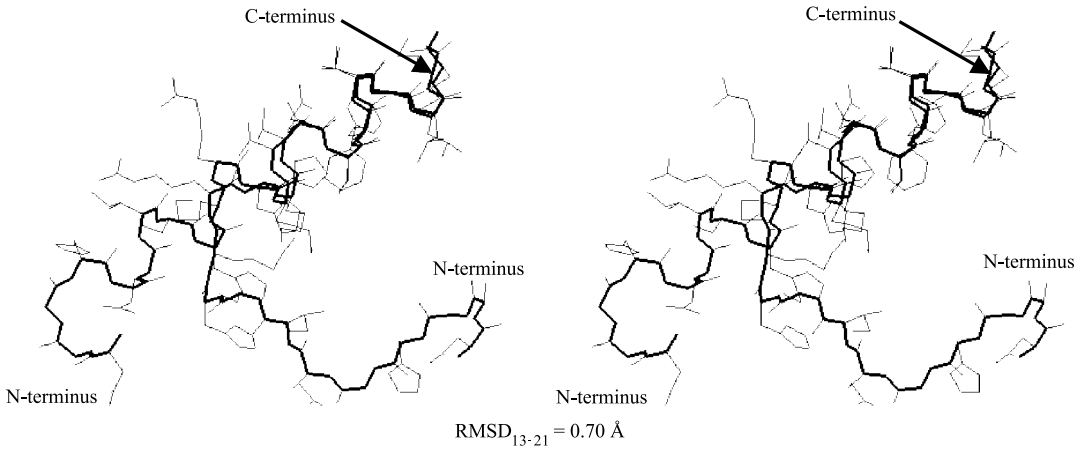

Figure 4 Stereoview of superposition of conformations of NPγ molecule with statistical weights higher than 3% in DMSO-d_6 obtained in ECEPP/3 force field. Superposition in Lys13–Met21 fragment was calculated (RMSD = 0.70 Å). Backbones are represented by the bold line.

Table 3 Measured and Computed Values of the Vicinal Coupling Constants $^3J_{NHH}\alpha$ of NPγ

Residue	Experimental $^3J_{NHH\alpha}$ vicinal coupling constants	EDMC ensemble 1.37[a] 55.26[b]	SA (AMBER4.1) ensemble 0.46[a] 27.88[b]	SA (X-PLOR) ensemble 0.528[a] 28.53[b]
	J_{exp}[Hz]	J_{calc}[Hz]	J_{calc}[Hz]	J_{calc} [Hz]
Gln6	8.1	7.02	8.54	7.57
Ile7	8.0	7.49	7.01	8.01
Ser8	8.3	7.19	8.16	8.15
His9	8.1	6.76	8.15	8.13
Lys10	6.6	7.02	6.66	7.78
Lys13	8.4	7.40	8.52	7.71
Thr14	8.0	7.35	7.87	7.96
Asp15	9.0	7.07	8.60	8.60
Phe17	9.2	10.04	8.97	8.87
Leu20	7.3	9.94	7.27	7.56
Met21	7.2	9.04	8.16	7.91

[a] Standard deviation in coupling constant.
[b] Standard deviation in peak volume.

changed by no more than 10%. It should be realized, however, that the selected representative conformations do not constitute the entire conformational ensemble.

Molecular structures have been drawn and analysed with the MOLMOL program [35].

RESULTS AND DISCUSSION

As shown in Figure 1, the CD spectrum of NPγ in TFE has two minima at 208 nm, and about 220 nm, respectively, indicating the presence a helical structure in this solvent. The CD spectra recorded in water, TFE aqueous solutions, phosphate buffer and in the presence of SDS micelles were very similar displaying a minimum at about 200 nm and a maximum at shorter wavelengths. The spectra suggest the lack of any preferential conformation(s) of NPγ under these conditions. The CD experiments revealed that although the peptide studied is conformationally flexible in polar solvents, a strong tendency to adopt a helical structure was observed when NPγ entered the hydrophobic environment. For obvious reasons (strong absorbance in the UV region) DMSO cannot be applied for CD investigations. The most frequently utilized solvents for the determination of the solution structure of bioactive peptides in the NMR experiments are water, aqueous buffers and DMSO. From CD experiments we know that aqueous solvent systems do not induce a secondary structure of NPγ. Therefore we decided to use DMSO, which is believed to imitate the receptor's environment. This solvent was also used in conformational studies of other tachykinins and other bioactive peptides.

NMR study of NPγ was performed in DMSO-d_6. The chemical shifts of the protons and vicinal coupling constants are summarized in Table 1. For the peptide studied, one distinct set of residual proton resonances in all spectra is displayed. All peptide bonds were found to be in *trans* configuration.

Figure 2 shows the NOE effects patterns obtained for the peptide studied. Strong NOE effects for H^{α}_{i}-HN_{i+1} connectivities through the whole molecule, and HN_i-HN_{i+1} in the *C*-terminal fragment were found. The presence of NOE effects observed for sequential connectivities between HN_i-HN_{i+1}, and also (HN, H^{α}, H^{β})$_i$-HN_{i+3}, H^{α}_{i}-HN_{i+4}, H^{α}_{i}-$H^{\alpha}_{i+3,i+4}$ and H^{α}_{i}-HN_{i+5} indicate a helical or reverse structure in the Ile7-His12 fragment. Additionally, one long-range NOE HN-H^{β} for Asp1 and Lys13 protons was found, which also confirms a reverse structure of the NPγ molecule. On the other hand, the values of vicinal coupling constants (Table 1) are about 8 Hz, indicating conformational flexibility of NPγ in DMSO-d_6 solution. Therefore, the final conclusion about the three-dimensional of NPγ has been drawn based on the calculations using NMR data.

The calculations with the X-PLOR program with the applied NMR constrains resulted in nine families of conformations for the peptide studied (Table 2). The RMSD of the lowest-energy structures from each family obtained for all C^{α} atoms is 3.19 Å (Figure 3a). All of them are stabilized by several β-turns. The common structural motif is a type IV β-turn in the Gln6–His12 fragment. It is worth noting that most of the conformations (291 of 300 computed) belong to the first family. The superposition of the 10 lowest-energy conformers of the first family is shown in Figure 3b (RMSD = 1.03 Å, obtained for all C^{α} atoms). They adopt very similar shapes in the middle region of the molecule.

In the case of the second applied method, the results obtained suggest that most of NPγ conformations, generated with the ECEPP/3 + SRFOPT force field, contain helical structure. Only two conformations with similar shapes having statistical weights higher than 3% were obtained (Table 2). Both contain a very high content of α-helix. They superimpose especially well in the Lys13–Met21 fragment (RMSD = 0.71 Å, obtained for C^{α} atoms) (Figure 4). The dominant conformation (62%) forms an α-helix in the *C*-terminal part (Lys13–Met21) of the molecule. Moreover the *N*-terminal and *C*-terminal fragments are close. The second conformer (32%) forms α-helical structure in the Gln6–Met21 fragment. We also performed calculations using surface model solvation parameters derived for polypeptides in DMSO [36] but the results were very similar (not shown) to those obtained with atomic solvation parameters of the SRFOPT model. It is known [37] that the ECEPP/3 force field biases generation for some peptide conformations a higher content of α-helix compared with *ab initio* calculations. Therefore the application of this force field for the conformational study of NPγ is rather limited.

A significantly more diverse set of conformations was obtained in the case of the AMBER4.1 force field with Simulated Annealing protocol. The best fit to the experimental NOESY spectrum was obtained after superposition of 14 low-energy conformations in which statistical weights were higher than 3% (Table 2). The calculated statistical weights of these conformations were in the range 9.3%–3.3%. None of them can be considered as the dominant one.

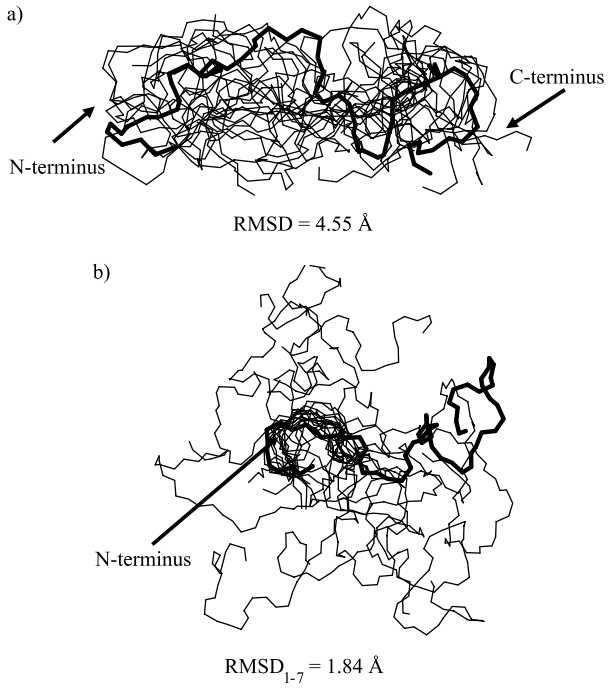

Figure 5 Superposition of conformations of NPγ molecule with statistical weights higher than 3% in DMSO-d_6 obtained in the AMBER4.1 force field obtained (a) for all α-carbon atoms (RMSD = 4.55 Å) and (b) for α-carbon atoms in the Asp1-Ile7 fragment (RMSD = 1.84 Å). Backbone of the most populated conformation is represented by the bold line.

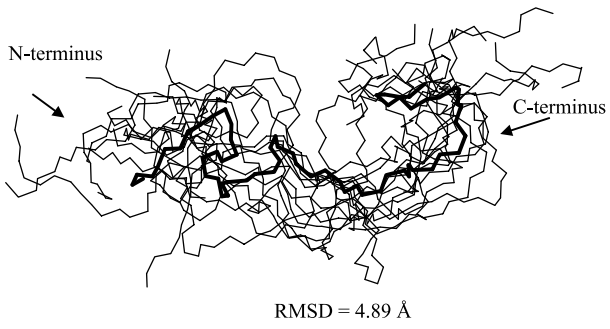

Figure 6 Superposition of conformations obtained using the Simulated Annealing protocol in CHARMM force field (without constraints put on proton distances and dihedral angles) implemented in X-PLOR program; for all α-carbon atoms RMSD = 4.89 Å.

The superposition of all conformations in all α-carbons yields RMSD = 4.55 Å (Figure 5a), which indicates the conformational flexibility of the peptide studied. More similar appeared to be fragments 1–7 (Figure 5b), 7–13 and 13–21. The calculated RMSDs in all cases were about 2 Å (not shown). In all conformations several β-turns were calculated and in some cases also γ-turns were found. But in fact, it is rather difficult to select the position of the secondary element(s) present in the solution structure of NPγ. The comparison of measured and computed values of vicinal constants $^3J_{HNH}\alpha$ and standard deviations (Table 3) for conformations obtained by EDMC and molecular dynamic protocols indicate that in the AMBER4.1 force field computed conformations fit better to the experimental data.

All conformers obtained in CHARMM force field revealed some similarities to those obtained in the AMBER force field. Superposition of conformers with statistical weights higher than 3% gave RMSD = 4.89 Å (Figure 6). The range of statistical weights was 9.6%–3.2%. The calculated coupling constants are summarized in Table 3. In most cases some β- and γ-turns were found (Table 2) but we could not determine the exact position of the dominant secondary element(s). The conformation with the highest statistical weight of 6.5% is similar to one with the highest statistical weight obtained with the AMBER4.1 force field (Figure 7a). The *C*-terminal fragments are in good agreement RMSD = 1.73 Å (Figure 7b) in particular.

CONCLUSIONS

In the present work we studied the solution structure of NPγ in DMSO-d_6 using two different methods. In the second method three different force fields were used. We showed that application of the ECEPP force field in this particular case is rather limited. All conformations calculated contain an unusually high content of α-helix. Diverse sets of conformations were calculated and selected by the AMBER4.1 and CHARMM force fields and the second approach. Nevertheless the comparison of the lowest-energy conformation calculated by the X-PLOR program using NMR constraints at the stage of structure calculations and the conformation with the highest statistical weight (9.3%) calculated in AMBER4.1 and CHARMM force fields revealed certain similarities in their backbones (Figure 7a), especially in their *C*-terminal 13–21 fragments (Figure 7b). Taking into consideration the differences in these two approaches (the ANALYZE program was designed to study the conformational equilibrium in a solution of peptides, whereas the X-PLOR program was originally dedicated to conformational studies of rather large proteins with small conformational freedom) the conformations

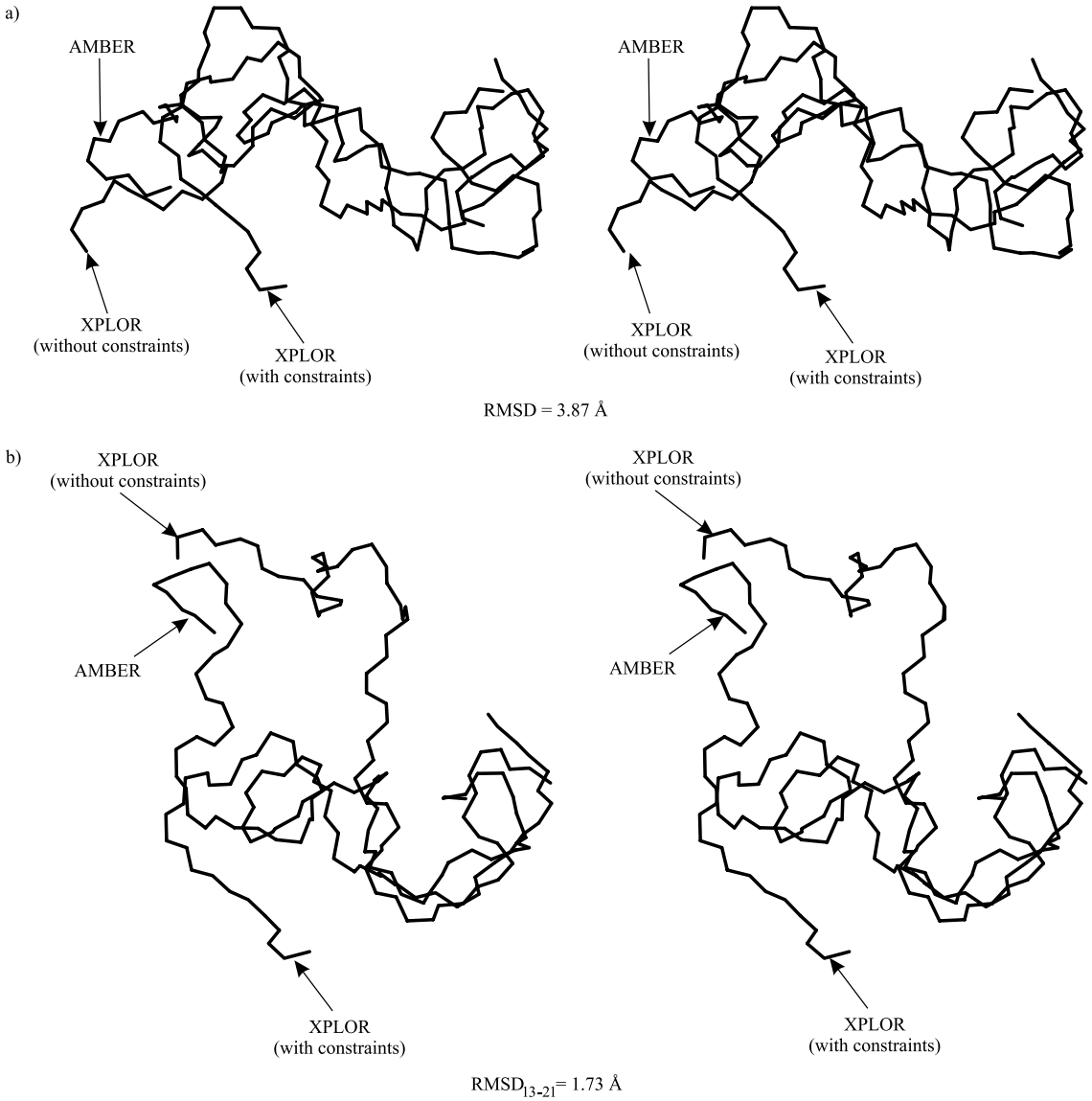

Figure 7 Stereoview of backbones superposition of the highest statistical weight conformation obtained in AMBER and CHARMM force field and one obtained in X-PLOR SA protocol (a) superposition of the whole backbone RMSD = 3.87 Å; (b) superposition of fragment 13-21 RMSD = 1.73 Å.

selected reflect the nature of NPγ under the conditions used in the NMR experiment. Nevertheless all conformations obtained in the two approaches adopt similar turn shapes in the middle region of the molecule and a random structure on the *N*- and *C*-terminal fragments. The sequence of the *C*-terminal NPγ decapeptide is identical with the sequence of NKA. Both peptides display preferable agonistic activity towards the NK-2 tachykinin receptor, although their pharmacological profiles are different. There are also differences in their conformational behaviour in solution. As reported by Whitehead *et al.* [9]. NKA adopts a helical structure in SDS micelles but we did not observe such a secondary structure formation for NPγ. In addition, the folded structures reported for NKA in solutions are different from those observed in the case of NPγ .

Acknowledgements

This work was supported by the Polish State Committee for Scientific Research (KBN), grant No. PB463/T09/97/13. The calculations were carried out in the Academic Computer Centre (TASK) in

Gdańsk, Poland, and Interdisciplinary Center for Mathematical Modeling (ICM) in Warsaw, Poland.

We acknowledge the help of Dr Igor Zhukov from the Institute of Biochemistry and Biophysics Polish Academy of Sciences, Warsaw in the collection of ACT-ct-COSY spectrum.

S. R-M. is a stipendist of the Foundation for Polish Science for young scientists.

REFERENCES

1. Kage R, McGregor GP, Thim L, Conlon JM. Neuropeptide-gamma: a peptide isolated from rabbit intestine that is derived from gamma-preprotachykinin. *J. Neurochem.* 1988; **50**: 1412–1417.
2. Polidori C, Staffinati G, Pefrumi MC, De Caro G, Massi M. Neuropeptide gamma: a mammalian tachykinin endowed with potent antidipsogenic action in rats. *Physiol. Behav.* 1995; **58**: 595–602.
3. Reynolds AM, Reynolds P, Holmes M, Scicchitano R. Tachykinin NK2 receptors predominantly mediate tachykinin-induced contractions in ovine trachea. *Eur. J. Pharmacol.* 1998; **12**: 211–223.
4. Nsa Allogho S, Nguyen-Le XK, Gobeil F, Pheng LH, Regoli D. Neurokinin receptors (NK1, NK2) in the mouse: a pharmacological study. *Can. J. Physiol. Pharmacol.* 1997; **75**: 552–557.
5. Burcher E, Alouan LA, Johnson PR, Black JL. Neuropeptide gamma, the most potent contractile tachykinin in human isolated bronchus, acts via a 'non-classical' NK2 receptor. *Neuropeptides* 1991; **20**: 79–82.
6. Chassaing G, Convert O, Lavielle S. Conformational Study of Neurokinin A: Comparison with Substance P and Physalaemin. *Peptides 1986, Proc. 19th European Peptide Symposium*, Theodoropoulos D (ed.). Walter de Gruyter: Berlin-New York, 1987; 303–306.
7. Horne J, Sadek M, Craik DJ. Determination of the solution structure of neuropeptide K by high-resolution nuclear magnetic resonance spectroscopy. *Biochemistry* 1993; **32**: 7406–7412.
8. Saviano G, Temussi PA, Motta A, Maggi CA, Rovero P. Conformation–activity relationship of tachykinin neurokinin A (4–10) and of some [Xaa^8] analogues. *Biochemistry* 1991; **30**: 10 175–10 181.
9. Whitehead TL, McNair S, Hadden CE, Young JK, Hicks RP. Membrane-induced secondary structures of neuropeptides: a comparison of the solution conformations adopted by agonists and antagonists of the mammalian tachykinin NK_1 receptor. *J. Med. Chem.* 1998; **41**: 1497–1506.
10. Sole NA, Barany G. Optimization of solid-phase synthesis of [Ala^8]-dynorphin-A. *J. Org. Chem.* 1992; **57**: 5399–5403.
11. Koźmiński W. The new active-coupling-pattern tilting experiment for an efficient and accurate determination of homonuclear coupling constant. *J. Magn. Res.* 1998; **134**: 189–193.
12. Bax A, Davis DG. Assignment of complex ^{1}H NMR spectra via two-dimensional homonuclear Hartmann-Hahn spectroscopy. *J. Am. Chem. Soc.* 1985; **107**: 2820–2821.
13. Bax A, Davis DG. Practical aspects of two-dimensional transverse NOE spectroscopy. *J. Magn. Reson.* 1985; **63**: 207–213.
14. Jeener J, Meier BH, Bachmann P, Ernst RR. Investigation of exchange processes by two-dimensional NMR spectroscopy. *J. Chem. Phys.* 1979; **71**: 4546–4553.
15. Bax A, Griffey R, Hawkins BL. Sensitivity enhanced correlation of ^{15}N and ^{1}H chemical shifts in natural abundance samples via multiple quantum coherence. *J. Am. Chem. Soc.* 1983; **105**: 7188–7190.
16. Summers MF, Marzilli LG, Bax A. Complete ^{1}H and ^{13}C assignments of coenzyme-B12 through the use of new two dimensional NMR experiments *J. Am. Chem. Soc.* 1986; **108**: 4285–4294.
17. Bartles C, Xia T, Billeter M, Güntert P, Wütrich K. The program XEASY for the computer-supported NMR spectral analysis of biological macromolecules. *J. Biomol. NMR* 1995; **5**: 1–10.
18. Güntert P, Braun W, Billeter M, Wüthrich K. Automated stereospecific ^{1}H NMR assignments and their impact on the precision of protein structure determination in solution. *J. Am. Chem. Soc.* 1989; **111**: 3997–4004.
19. Güntert P, Wüthrich K. Improved efficiency of protein structure calculation NMR data using program DYANA with redundant dihedral angle constraints. *J. Biomol. NMR* 1991; **1**: 447–456.
20. Bystrov VF. Spin-spin coupling and the conformational states of peptide systems. *Progr. NMR Spectrosc.* 1976; **10**: 41–81.
21. Güntert P, Wüthrich K. Efficient computation of three-dimensional protein structures in solution from nuclear magnetic resonance data using the program DYANA and the supporting programs CALIBA, HABAS and GLOMSA. *J. Mol. Biol.* 1991; **217**: 517–530.
22. Groth M, Malicka J, Czaplewski C, Liwo A, Łankiewicz L, Wiczk W. Maximum entropy approach to the determination of solution conformation of flexible polypeptides by global conformational analysis and NMR spectroscopy — Application to DNS^1-c[D-A_2bu^2, Trp^4, Leu^5]-enkephalin and DNS^1-c[D-A_2bu^2, Trp^4, D-Leu^5]-enkephalin. *J. Biomol. NMR* 1999; **15**: 315–330; http://www.tc.cornell.edu/resource/CompBiology Tools/analyze.
23. Ripoll DR, Scheraga HA. On the multiple-minima problem in the conformational analysis of polypeptides. II. An electronically driven Monte Carlo method-tests on poly(L-alanine). *Biopolymers* 1988; **27**: 1283–1303.

24. Némethy G, Gibson KD, Palmer KA, Yoon CN, Paterlini G, Zagari A, Rumsey S, Scheraga HA. Energy parameters in polypeptides. 10. Improved geometrical parameters and nonbonded interactions for use in the ECEPP/3 algorithm with application to proline-containing peptides. *J. Phys. Chem.* 1992; **96**: 6472–6484.
25. Pearlman DA, Case JW, Caldwell JW, Ross W, Cheatham TE, Ferguson D, Seibel GL, Singh UC, Weiner P, Ollman PA. *AMBER4.1 Manual*. University of California: California, USA, 1995; 98–149.
26. Brünger AT. *The X-PLOR Software Manual*. Version 3.1. Yale University Press: New Haven, CT, 1992.
27. Brooks B, Bruccoleri R, Olafson BO, States DJ, Swaminathan S, Karplus M. CHARMM a program for macromolecular energy, minimization and dynamics calculations. *Comp. Chem.* 1983; **4**: 187–217.
28. Powell MJD. Restart procedures for conjugate gradient method program. *Math. Prog.* 1977; **12**: 241–254.
29. Vila J, Williams RL, Vásquez M, Scheraga HA. Empirical solvation models can be used to differentiate native from near-native conformations of bovine pancreatic trypsin inhibitor. *Proteins Struct. Funct. Genet.* 1991; **10**: 199–218.
30. Ripoll DR, Pottle MS, Gibson KD, Liwo A, Scheraga HA. Implementation of the ECEPP algorithm, the Monte Carlo minimization method. *J. Comput. Chem.* 1995; **16**: 1153–1163.
31. Späth H. Cluster analysis algorithms. *J. Comput Chem.* 1980; **10**: 209–220.
32. Massefski W Jr, Bolton PH. Quantitative analysis of nuclear Overhauser effects. *J. Magn. Reson.* 1985; **65**: 526–530.
33. Meadows RP, Post CB, Luxon BA, Gorenstein DG. *MORASS 2.1*. Purdue University: West Lafayette, 1994.
34. Post CB, Meadows RP, Gorenstein DG. On the evaluation of interproton distance for 3-dimensional structure determination by NMR using a relaxation rate matrix analysis. *J. Am. Chem. Soc.* 1990; **112**: 6796–6803.
35. Koradi R, Billeter M, Wütrich K. MOLMOL: a program for display and analysis of macromolecular structures. *J. Mol. Graphics* 1996; **14**: 51–55.
36. Groth M, Malicka J, Rodziewicz-Motowidło S, Czaplewski C, Bunda L, Wiczk W, Liwo A. Determination of conformational equilibrium of peptides in solution by NMR spectroscopy and theoretical conformational analysis: application to the calibration of mean-field solvation models. *Biopolymers* 2001; **60**: 79–95.
37. Ołdziej S, Dobrzańska U, Liwo A. ECCC7 Electronic Computional Chemistry Conference, Poster 41, April 2001; http://eccc7.cooper.edu

